Increased gene dosage of the *Ink4/Arf* locus does not attenuate atherosclerosis development in hypercholesterolaemic mice

José J. Fuster [a, *], Pedro Molina-Sánchez [a, *], David Jovaní [b], Ángela Vinué [b], Manuel Serrano [c], Vicente Andrés [a]

[a] Department of Epidemiology, Atherothrombosis and Imaging, Centro Nacional de Investigaciones Cardiovasculares (CNIC), Melchor Fernández Almagro 3, 28029 Madrid, Spain.

[b] Department of Molecular and Cellular Pathology and Therapy, Instituto de Biomedicina de Valencia-Consejo Superior de Investigaciones Científicas (IBV-CSIC), Jaime Roig 11, 46010 Valencia, Spain.

[c] Spanish National Cancer Research Center (CNIO), Melchor Fernández Almagro 3, 28029 Madrid, Spain.

* Authors with equal contribution

Corresponding author:

Vicente Andrés

CNIC, Melchor Fernández Almagro 3, 28029 Madrid, Spain.

Telephone: +34-914531200 (ext. #1502) FAX: +34-914531262

e-mail: vandres@cnic.es

ABSTRACT

Rationale. Human genome-wide association studies have identified genetic variants in the chromosome 9p21 region that confer increased risk of coronary artery disease and other age-related diseases. These variants are located in a block of high linkage disequilibrium with the neighbouring *Ink4/Arf* tumour-suppressor locus (also named *CDKN2A/CDKN2B*). Since previous studies suggest an atheroprotective role of the *Ink4/Arf* locus, here we assessed whether gain-of-function of the encoded genes can be exploited therapeutically to reduce atherosclerosis.

Methods. Generation and characterization of apolipoprotein E-null mice carrying an additional transgenic copy of the entire *Ink4/Arf* locus (apoE-/-Super-Ink4/Arf) that reproduces the normal expression and regulation of the endogenous locus.

Results. Although liver and aorta of apoE-/-Super-Ink4/Arf mice only showed a trend towards increased *Ink4/Arf* transcript levels compared to apoE-/- controls, cultured macrophages with increased *Ink4/Arf* gene dosage exhibited augmented apoptosis induced by irradiation with ultraviolet light, indicating that low level of transgene overexpression can lead to augmented *Ink4/Arf* function. However, increased *Ink4/Arf* gene dosage did not affect atherosclerosis development in different vascular regions of both male and female apoE-/- mice fed either normal or high-fat diet. Increased gene dosage of *Ink4/Arf* similarly had no effect on atheroma cell composition or collagen content, an index of plaque stability.

Conclusion. In contrast with previous studies demonstrating cancer resistance in Super-Ink4/Arf mice carrying an additional transgenic copy of the entire *Ink4/Arf* locus, our results cast doubt on the potential of *Ink4/Arf* activation as a strategy for the treatment of atherosclerotic disease.

Keywords: Ink4/Arf, CDKN2A/B, $p15^{Ink4b}$, $p16^{Ink4a}$, 9p21, atherosclerosis

INTRODUCTION

Atherosclerosis and associated ischemic events are the leading cause of morbidity and mortality in industrialized countries. Atherosclerotic plaque development is a multifactorial chronic inflammatory process characterized by increased neointimal cell proliferation [1], senescence [2] and apoptosis [3], which is affected by both environmental and genetic factors. Recent genome-wide association studies have demonstrated that certain common single-nucleotide polymorphisms (SNPs) in the chromosome 9p21 region confer increased risk of coronary artery disease and other atherosclerotic conditions in humans [4-12]. The core region of the 9p21 atherosclerosis risk haplotype contains no protein coding genes, but is located in a block of high linkage disequilibrium with the neighbouring *Ink4/Arf* locus, which includes the cyclin-dependent kinase (CDK)-inhibitory genes *CDKN2A* (encoding $p16^{Ink4a}$) and *CDKN2B* (encoding $p15^{Ink4b}$), and the *CDKN2A* alternative reading-frame transcript *Arf* (human $p14^{Arf}$, mouse $p19^{Arf}$). Moreover, the 9p21 risk region overlaps with the sequence that produces *ANRIL* (Antisense Noncoding RNA in the *Ink4* Locus), a large non-coding RNA with multiple splice variants whose expression is associated with the 9p21 genotype [13-17].

The mechanisms by which the 9p21 locus affects atherosclerosis development remain incompletely understood. It is noteworthy that the *CDKN2A* and *CDKN2B* genes are tumour suppressors that regulate several cellular processes that contribute to atherosclerosis development, including cell proliferation and apoptosis [18]. $p16^{Ink4a}$ and $p15^{Ink4b}$ are negative regulators of cell proliferation that block cell-cycle progression by inhibiting cyclin D-containing CDK4,6 complexes and the ensuing accumulation of hypophosphorylated retinoblastoma protein. Arf suppresses growth and promotes apoptosis by stabilizing p53 through inhibition of the ubiquitin ligase MDM2. Remarkably, $p16^{Ink4a}$, $p15^{Ink4b}$ and Arf are expressed in human atherosclerotic plaques [19], and some studies in blood cells have found a significant association between altered expression of *Ink4/Arf* transcripts and certain high-risk SNPs within the 9p21 region [15, 17]. These findings support the possibility that impaired *Ink4/Arf* gene expression is involved in the increased atherosclerosis susceptibility associated with the 9p21

risk haplotype. Consistent with this notion, *ANRIL* has been shown to directly repress the expression of the *Ink4/Arf* locus [20, 21], and deletion of a 70-kb non-coding region on mouse chromosome 4, orthologous to the human 9p21 locus, greatly reduces cardiac expression of the murine *CDKN2A* and *CDKN2B* genes [22]. However, given the complexity of the *Ink4/Arf* locus and the multiplicity of *ANRIL* variants, further studies are required to establish a clear link between the 9p21 region and disturbed expression or function of *Ink4/Arf* gene products [12, 23].

Regardless of the molecular connection between 9p21 and *Ink4/Arf* expression, animal studies strongly support a role of the encoded genes in vasculoproliferative disease. Local delivery of $p15^{Ink4b}$ significantly inhibits in-stent neointimal hyperplasia in a rabbit angioplasty model [24]. Moreover, we have shown that whole-body ablation of *Arf* reduces apoptosis of neointimal macrophages and vascular smooth muscle cells (VSMCs) and accelerates atherosclerosis in hypercholesterolaemic apolipoprotein E-null (apoE-/-) mice [25]. More recently, Kuo et al. [26] reported that transplantation of bone marrow-derived cells with $p16^{Ink4a}$ and *Arf* deficiency into irradiated cholesterol-fed low-density lipoprotein receptor (LDLR)-deficient mice accelerates atherosclerosis, coinciding with increased monocyte/macrophage proliferation. Likewise, primary VSMCs lacking the 70-kb non-coding region on mouse chromosome 4 orthologous to the human 9p21 locus exhibit excessive proliferation [22]. While these studies suggest an atheroprotective role for the *Ink4/Arf* locus, they leave unanswered the question of whether gain-of-function of the encoded genes can be exploited therapeutically to reduce atherosclerosis. In this study, we approach this question by analysing atherosclerosis development in apoE-/- mice with increased dosage of the murine *Ink4/Arf* locus (apoE-/-Super-Ink4/Arf).

METHODS

Mice, diet, and metabolic measurements. Care and manipulation of mice was in accordance with European Commission guidelines and was approved by institutional ethics review board. Transgenic Super-Ink4/Arf mice carrying one extra transgenic copy of the entire *Ink4/Arf* locus [27] were backcrossed for more than 8 generations in a C57BL/6J background and then interbred with apoE-/- mice (C57BL/6J, Charles River) to generate apoE-/-Super-Ink4/Arf mice. For the analysis of native atherosclerosis, apoE-/- and apoE-/-Super-Ink4/Arf mice were maintained on a low-fat standard diet (2.8% fat; Panlab) and were sacrificed at eight months of age. For diet-induced atherosclerosis, 2-month-old mice were challenged for 10 weeks with a high-fat atherogenic diet (10.8% total fat, 0.75% cholesterol, S4892-E010, SSNIFF). Plasma lipid levels in overnight-fasted mice were measured by enzymatic procedures (WAKO). The number of mice included in each study is indicated in the legends of the figures.

Gene expression analysis by quantitative real-time PCR (qPCR). RNA was obtained from murine liver and aorta (aortic arch and thoracic aorta) using TRIzol Reagent (Invitrogen). After verification of purity and concentration by the A260/280 ratio, RNA (0.5-1µg) was retro-transcribed with High Capacity cDNA Reverse Transcription Kit and amplified using Power SYBER green master mix (both from Applied Biosystems). The following primers (Forward: Fw; Reverse: Rv) designed with the Primer Express software (Applied Biosystems) were used (mouse sequences):

Ink4a: Fw-5'-CGAACTCTTTCGGTCGTACCC-3'; Rv-5'-TTGAGCAGAAGAGCTGCTACG-3'

Ink4b: Fw-5'-AGATCCCAACGCCCTGAACC-3'; Rv-5'-ACAGGTCTGGTAAGGGTGGC-3'

Arf: Fw-5'-TCTTGAGAAGAGGGCCGCACC-3'; Rv-5'-GAATCTGCACCGTAGTTGAGC-3'

Reactions were run on a thermal Cycler 7500 Fast System and results were analyzed with the software provided by the manufacturer (Applied Biosystems). Gene expression was normalized to housekeeping controls (GAPDH and 18S for liver and 18S for aorta).

Macrophage culture and apoptosis assay. Bone marrow-derived macrophages were obtained from suspensions of femoral bone marrow, plated at $1x10^6$ cells/mL and differentiated for 7d in DMEM supplemented with antibiotics, 10% fetal bovine serum and 10% L929-cell conditioned medium as a source of macrophage colony-stimulating factor. Macrophages were irradiated with ultraviolet (UV) light (80 J/m^2), and cultured for an additional 24h. Cells were trypsinized, washed with PBS, collected by centrifugation (5min, 400*g*), fixed with 80% ethanol (1h, -20°C), and labelled with propidium iodide (50 μg/ml) in the presence of RNase A (0.025 mg/ml) for 30min at room temperature. Apoptotic hypodiploid cells were detected using a BD FACSCanto Flow cytometer (BD Biosciences).

Atherosclerosis burden. Mice were sacrificed and the aorta was removed after *in situ* perfusion with PBS followed by 4% paraformaldehyde/PBS. Fixation was continued overnight at 4ºC. Whole aortas were stained with 0.2% Oil Red O in 80% methanol, and portions of aortic sinus and ascending aorta were paraffin-embedded to obtain cross-sections as described [25]. An operator blinded to genotype quantified the extent of atherosclerosis in Oil Red O-stained whole-mount tissue and in hematoxylin/eosin-stained cross-sections using computer-assisted morphometric analysis (SigmaScan Pro5, Aspire Software International). For each mouse, atherosclerosis burden in cross-sections was calculated as the average of 4 independent sections separated by ~6 μm.

Immunohistochemical analysis of atheroma. Immunohistopathological examination of atheromas was performed by a researcher blinded to genotype and included quantification of macrophage, VSMC, and collagen content. VSMCs were identified with alkaline-phosphatase-conjugated mouse anti-smooth muscle α-actin (SMα-actin) monoclonal antibody (1/25 dilution, clone 1A4) and Fast Red substrate (both from Sigma). Macrophages were identified with rat anti-Mac3 monoclonal antibody (1/200 dilution, clone M3/84, sc-19991, Santa Cruz Biotechnology), followed by incubation with biotin-conjugated goat anti-rat secondary antibody (1/300 dilution, sc-2041, Santa Cruz Biotechnology), streptavidin- HRP (TS-060-HR, Lab Vision Corporation) and DAB substrate (BUF021A, AbD Serotec). Collagen was detected by Masson´s trichrome staining. Tissue sections were counterstained with hematoxylin and images were acquired with an Olympus CAMEDIA-C5060 wide zoom digital camera (Olympus) mounted on an Axiolab stereomicroscope (Carl Zeiss). Collagen was quantified with Metamorph (Molecular Devices), and Mac3 and SMα-actin using ImageJ (National Institutes of Health).

Neointimal cell proliferation and apoptosis. Proliferation within atherosclerotic plaques was estimated by double staining with anti-Ki67 plus anti-F4/80 or anti-Ki67 plus anti-SMα-actin to identify proliferating macrophages and VSMCs, respectively. After deparaffinization, antigen retrieval and blockade of non-specific interactions (5% horse serum in PBS, 45min), histological sections were incubated for 2h at 37º C with anti-Ki67 antibody (prediluted, Clone SP6; Vitro) together with anti-F4/80 (1/100 dilution, MCA497G, AbD Serotec) or anti-SMα-actin (1/75 dilution,Cy3-conjugated, C6198, SIGMA). F4/80 was visualized with Alexa Fluor 488-conjugated secondary antibodies (A11006, Invitrogen) and Ki67 with Alexa Fluor 635-conjugated anti-rabbit IgG (A31577, Invitrogen). Plaque apoptosis was determined using the terminal deoxynucleotidyl transferase dUTP nick-end labelling (TUNEL) method, following the manufacturer's recommendations (In Situ Cell Death Detection Kit Fluorescein, Roche). Nuclei were stained with DAPI and slides were mounted in Slow-Fade Gold Antifade reagent to acquire images on a Leica SP5 confocal microscope fitted with a 40X oil-immersion objective. Settings were adjusted

to maximize the signal-to-noise ratio. The sequential mode was used for image acquisition in order to avoid any interference from overlapping fluorescence. Images were analyzed with Metamorph by a researcher who was blinded to genotype.

Data analysis. Results are expressed as means±SE. In experiments with two groups, statistical significance was evaluated with a 2-tailed, unpaired *t*-test. Otherwise, a two-way ANOVA with Bonferroni's post-hoc test was used (GraphPad Prism software). A value of $p<0.05$ was considered significant.

RESULTS

Atherosclerosis development in fat-fed apoE-/- and apoE-/-Super-Ink4/Arf mice. To assess whether increased *Ink4/Arf* gene dosage protects against atherosclerosis development, we crossed atherosclerosis-prone apoE-/- mice with Super-Ink4/Arf mice to generate apoE-/- mice with either normal *Ink4/Arf* gene dosage or with an extra transgenic allele of the entire endogenous locus (apoE-/-Super-Ink4/Arf mice). Previous studies have shown that Super-Ink4/Arf mice regulate transgene expression similarly to the endogenous gene, exhibiting moderately increased $p16^{Ink4a}$, $p15^{Ink4b}$ and $p19^{Arf}$ expression in a number of tissues at old ages (~1.5-year-old mice) [27]. Likewise, the basal levels of $p16^{Ink4a}$ and $p19^{Arf}$ were only modestly increased in mouse fibroblasts obtained from Super-Ink4/Arf embryos [28]. Consistent with these previous studies, we observed a modest upregulation of Ink4/Arf transcript levels in liver and aorta of 4-8-month-old apoE-/-Super-Ink4/Arf mice compared to age-matched apoE-/- controls (Fig.1A). Although differences only reached statistical significance in Ink4b expression in liver, we found higher UV-induced apoptosis in macrophages derived from apoE-/-Super-Ink4/Arf bone marrow than in apoE-/- cells, suggesting increased functionality of the Ink4/Arf transgene in spite of its low level of expression (Fig.1B). We next analysed atheroma size in different vascular regions of female mice that had been fed a high-fat diet for 10 weeks. Fat-feeding significantly increased circulating levels of cholesterol and triglycerides, with no differences observed between genotypes (Fig.2A). Atheroma size was also comparable between female apoE-/- and apoE-/-Super-Ink4/Arf mice, as revealed by examination of whole-mount oil Red-O–stained aortic arch and thoracic aorta (Fig.2B), and hematoxylin/eosin-stained cross-sections of aortic sinus and ascending aorta (Fig.2C). Similarly, the atherosclerosis burden in the aortic arch, thoracic aorta and aortic sinus was indistinguishable in fat-fed apoE-/- and apoE-/-Super-Ink4/Arf males (Fig.S1, online supplement). Immunohistological examination of plaque composition in the aortic sinus of males and females also revealed no differences between genotypes in lesional content of Mac3-immunoreactive macrophages, SMα-actin-immunoreactive VSMCs or collagen (Fig.3).

Atherosclerosis development in apoE-/- and apoE-/-Super-Ink4/Arf mice fed standard chow. To investigate the consequences of increased gene dosage of Ink4/Arf on atherosclerosis development under a less atherogenic setting, we examined 8-month-old apoE-/- and apoE-/-Super-Ink4/Arf mice fed standard low-fat chow. These studies revealed similar plasma lipid levels (Fig.4A) and comparable atheroma size in the aortic arch (Fig.4B) and aortic sinus of mice of both genotypes (Fig.4C). The relative plaque content of macrophages and collagen was also comparable in apoE-/- and apoE-/-Super-Ink4/Arf mice (Fig.4D). However, we observed a slight increase in VSMC content in atherosclerotic plaques of apoE-/-Super-Ink4/Arf mice fed standard chow that just reached statistical significance ($p= 0.0471$) (Fig.4D).

Increased gene dosage of the *Ink4/Arf* locus does not affect neointimal cell proliferation or apoptosis. The size and stability of atherosclerotic lesions are both determined by the balance between cell proliferation and apoptosis. Given the important role of the *Ink4/Arf* locus in regulating these processes, we measured cell proliferation and apoptosis in plaques from 8-month-old apoE-/- and apoE-/-Super-Ink4/Arf mice fed standard chow. Double immunofluorescence studies revealed similar percentage of neointimal proliferating macrophages (Ki67-F4/80 double-positive cells) (Fig.5A) and VSMCs (Ki67-SMα-actin double-positive cells) (Fig.5B) in both genotypes. To assess plaque apoptosis, aortic sinus cross-sections were examined using the TUNEL method. Only 1.2-1.5% of total cells were TUNEL-positive in apoE-/- and apoE-/-Super-Ink4/Arf atheromata, and average values did not display statistically significant differences between genotypes (Fig.5C).

DISCUSSION

Recent studies have identified common SNPs in a region of chromosome 9p21 near the *Ink4/Arf* locus that confer increased risk of atherosclerotic disease [4-12]. Although animal studies suggest that expression of $p16^{Ink4a}$ and *Arf* protect against atherosclerosis [25, 26], it remains to be determined whether the *Ink4/Arf* locus can be manipulated to inhibit disease development. We approached this question by analysing the effects of increased *Ink4/Arf* gene dosage on the development of atherosclerosis in hypercholesterolaemic apoE-/- mice. For this, we interbred apoE-/- mice with Super-Ink4/Arf mice that carry one extra transgenic copy of the entire *Ink4/Arf* locus [27]. We find a trend towards augmented Ink4/Arf transcript levels in liver and aorta of apoE-/-Super-Ink4/Arf mice aged 4-8 months compared to age-matched apoE-/- controls, but differences only reached statistical significance in hepatic Ink4b expression. Such modest response in apoE-/-Super-Ink4/Arf mice is in agreement with previous studies demonstrating that Ink4/Arf expression is only moderately increased in fibroblasts obtained from Super Ink4/Arf mouse embryos [28] and in tissues from ~1.5-year-old Super-Ink4/Arf mice [27], consistent with age-dependent increase in Ink4/Arf expression [29]. Importantly, low level of Ink4/Arf transgene expression confers cancer resistance in Super-Ink4/Arf mice without affecting normal viability or aging [27], and significantly augments nitric oxide-dependent apoptosis and caspase 3 activity in cultured Super-Ink4/Arf mouse embryonic fibroblasts [28]. Similarly, transgenic Super-p53 mice carrying an extra allele of the endogenous p53 gene do not exhibit significantly higher levels of p53 but have increased p53 functionality, as suggested by augmented apoptotic response to DNA damage [30, 31]. We also find higher UV-induced apoptosis in apoE-/-Super-Ink4/Arf bone marrow-derived macrophages than in apoE-/- controls, suggesting that the transgene leads to augmented Ink4/Arf function in spite of its low level of expression. However, increased Ink4/Arf gene dosage does not attenuate atherosclerosis development, since atherosclerotic plaques in various vascular regions were of similar size in apoE-/- and in apoE-/-Super-Ink4-Arf mice, whether animals were fed a high-fat diet or standard chow. Moreover, macrophage, VSMC and collagen content in the atherosclerotic plaque were

also generally comparable in both genotypes, irrespective of dietary regimen, with the exception of a modest increase in VSMC content in the aortic sinus of apoE-/-Super-Ink4/Arf mice fed standard diet that just reached statistical significance (p= 0.047). Thus, low level of *Ink4/Arf* overexpression in transgenic mice carrying one extra transgenic copy of the *Ink4/Arf* locus can confer cancer resistance [27] but does not protect against atherosclerosis development.

Our in vitro studies demonstrated augmented UV-induced apoptosis in apoE-/-Super-Ink4/Arf bone marrow-derived macrophages compared to apoE-/- controls. However, despite that 70-80% of apoptotic cells in apoE-/- lesions are macrophages [25], we did not observe differences in TUNEL staining when comparing plaques of both genotypes. Nonetheless, it should be noted that the percentage of TUNEL-positive neointimal cells in our in vivo studies was extremely low (apoE-/-: ~1.2%, apoE-/- Super-Ink4/Arf: ~1.5%), therefore it cannot be ruled out that differences between genotypes exist at disease stages featuring high level of apoptotic cell death. The observation that neointimal cell proliferation and apoptosis and atherosclerosis burden were unaffected in apoE-/-Super-Ink4/Arf mice was somewhat unexpected given that *Arf* gene ablation accelerates atherosclerosis development and reduces plaque apoptosis in apoE-/- mice [25], and that reduction of $p16^{Ink4a}$ and *Arf expression* in bone marrow-derived cells increases atherosclerosis development and monocyte/macrophage proliferation in transplanted LDLR-deficient mice [26]. It is possible that the moderate increase in *Ink4/Arf* expression achieved in apoE-/-Super-Ink4/Arf mice by introducing a single extra allele of the *Ink4/Arf* locus under the control of its own promoter is insufficient to enhance potential atheroprotective effects. Although the effect of higher level of Ink4/Arf expression could be tested, it is noteworthy that supraphysiological *Ink4/Arf* activation might provoke major noxious side effects, especially given that Ink4/Arf proteins appear to inhibit tissue regeneration in several settings [29, 32-34]. Another possibility is that, unlike $p16^{Ink4a}$ and *Arf,* $p15^{Ink4b}$ expression might promote atherosclerosis development in spite of its inhibitory effect against in-stent neointimal hyperplasia [24], so that the net effect of increasing activity of the entire *Ink4/Arf* locus in apoE-/-Super-Ink4/Arf mice is nil. A similar situation might pertain to the closely related CDK inhibitory

proteins $p21^{Cip1}$ and $p27^{Kip1}$, which inhibit neointimal thickening following angioplasty [35-38] but appear to play opposite roles in atherosclerosis development [39-41]. Moreover, distinct *Ink4/Arf* transcripts might exert different functions in the various cell types involved in atherosclerosis. Thus, before ruling out the utility of targeting the *Ink4/Arf* locus as a means of preventing or treating atherosclerotic disease, future studies are warranted to thoroughly analyse the consequences for atheroma progression of overexpressing each *Ink4/Arf*–encoded proteins individually and selectively in the different cell types that are present in atherosclerotic lesions (e.g., VSMCs, endothelial cells, macrophages, and T-cells).

ACKNOWLEDGMENTS

We thank M. J. Andrés-Manzano for help with tissue sectioning and figure preparation and S. Bartlett for English editing. This work was supported by the Spanish Ministry of Science and Innovation (MICINN) (grant number SAF2010-16044), the Instituto de Salud Carlos III (RECAVA, grant number RD06/0014/0021), and the Dr. Léon Dumont Prize 2010 from the Belgian Society of Cardiology (to V.A.). P.M. is supported by the FPU doctoral fellowship program of the MICINN. The CNIC is supported by the MICINN and the Pro-CNIC Foundation.

CONFLICT OF INTEREST

None.

REFERENCES

[1] Fuster JJ, Fernández P, González-Navarro H, et al. Control of cell proliferation in atherosclerosis: Insights from animal models and human studies. Cardiovasc Res 2010; 86:254-64.

[2] Minamino T, Komuro I. Vascular cell senescence: Contribution to atherosclerosis. Circ Res 2007; 100:15-26.

[3] Stoneman VE, Bennett MR. Role of apoptosis in atherosclerosis and its therapeutic implications. Clin Sci (Lond) 2004; 107:343-54.

[4] Broadbent HM, Peden JF, Lorkowski S, et al. Susceptibility to coronary artery disease and diabetes is encoded by distinct, tightly linked snps in the anril locus on chromosome 9p. Hum Mol Genet 2008; 17:806-14.

[5] McPherson R, Pertsemlidis A, Kavaslar N, et al. A common allele on chromosome 9 associated with coronary heart disease. Science 2007; 316:1488-91.

[6] Helgadottir A, Thorleifsson G, Manolescu A, et al. A common variant on chromosome 9p21 affects the risk of myocardial infarction. Science 2007; 316:1491-3.

[7] Samani NJ, Erdmann J, Hall AS, et al. Genomewide association analysis of coronary artery disease. N Engl J Med 2007; 357:443-53.

[8] Schunkert H, Gotz A, Braund P, et al. Repeated replication and a prospective meta-analysis of the association between chromosome 9p21.3 and coronary artery disease. Circulation 2008; 117:1675-84.

[9] The Wellcome Trust Case Control Consortium. Genome-wide association study of 14,000 cases of seven common diseases and 3,000 shared controls. Nature 2007; 447:661-78.

[10] Shen GQ, Li L, Rao S, et al. Four SNPs on chromosome 9p21 in a South Korean population implicate a genetic locus that confers high cross-race risk for

development of coronary artery disease. Arterioscler Thromb Vasc Biol 2008; 28:360-5.

[11] Tousoulis D, Briasoulis A, Papageorgiou N, et al. Candidate gene polymorphisms and the 9p21 locus in acute coronary syndromes. Trends Mol Med 2008; 14:441-9.

[12] Cunnington MS, Keavney B. Genetic mechanisms mediating atherosclerosis susceptibility at the chromosome 9p21 locus. Curr Atheroscler Rep 2011; 13:193-201.

[13] Holdt LM, Beutner F, Scholz M, et al. ANRIL expression is associated with atherosclerosis risk at chromosome 9p21. Arterioscler Thromb Vasc Biol 2010; 30:620-7.

[14] Jarinova O, Stewart AF, Roberts R, et al. Functional analysis of the chromosome 9p21.3 coronary artery disease risk locus. Arterioscler Thromb Vasc Biol 2009; 29:1671-7.

[15] Liu Y, Sanoff HK, Cho H, et al. Ink4/arf transcript expression is associated with chromosome 9p21 variants linked to atherosclerosis. PLoS One 2009; 4:e5027.

[16] Burd CE, Jeck WR, Liu Y, et al. Expression of linear and novel circular forms of an Ink4/Arf-associated non-coding RNA correlates with atherosclerosis risk. PLoS Genet 2010; 6:e1001233.

[17] Cunnington MS, Santibanez Koref M, Mayosi BM, et al. Chromosome 9p21 snps associated with multiple disease phenotypes correlate with anril expression. PLoS Genet 2010; 6:e1000899.

[18] Gil J, Peters G. Regulation of the INK4b-ARF-INK4a tumour suppressor locus: All for one or one for all. Nat Rev Mol Cell Biol 2006; 7:667-77.

[19] Holdt LM, Sass K, Gabel G, et al. Expression of Chr9p21 genes CDKN2b (p15(INK4b)), CDKN2a (p16(INK4a), p14(ARF)) and MTAP in human atherosclerotic plaque. Atherosclerosis 2011; 214:264-70.

[20] Yap KL, Li S, Muñoz-Cabello AM, et al. Molecular interplay of the noncoding rna anril and methylated histone h3 lysine 27 by polycomb cbx7 in transcriptional silencing of ink4a. Mol Cell 2010; 38:662-74.

[21] Kotake Y, Nakagawa T, Kitagawa K, et al. Long non-coding RNA ANRIL is required for the PRC2 recruitment to and silencing of $p15^{INK4B}$ tumor suppressor gene. Oncogene 2011; 30:1956-62.

[22] Visel A, Zhu Y, May D, et al. Targeted deletion of the 9p21 non-coding coronary artery disease risk interval in mice. Nature 2010; 464:409-12.

[23] Linsel-Nitschke P, Schunkert H. Chromosome 9p21 and coronary risk--the mystery continues. Atherosclerosis 2011; 214:257-8.

[24] Segev A, Nili N, Qiang B, et al. Inhibition of intimal hyperplasia after stenting by over-expression of p15: A member of the ink4 family of cyclin-dependent kinase inhibitors. J Mol Cell Cardiol 2011; 50:417-25.

[25] González-Navarro H, Abu Nabah YN, Vinué A, et al. $p19^{ARF}$ deficiency reduces macrophage and vascular smooth muscle cell apoptosis and aggravates atherosclerosis. J Am Coll Cardiol 2010; 55:2258-68.

[26] Kuo C-L, Murphy AJ, Sayers S, et al. Cdkn2a is an atherosclerosis modifier locus that regulates monocyte/macrophage proliferation. Arterioscler Thromb Vasc Biol 2011; 31:2483-92.

[27] Matheu A, Pantoja C, Efeyan A, et al. Increased gene dosage of ink4a/arf results in cancer resistance and normal aging. Gene Dev 2004; 18:2736-46.

[28] Zeini M, Traves PG, López-Fontal R, et al. Specific contribution of $p19^{ARF}$ to nitric oxide-dependent apoptosis. J Immunol 2006; 177:3327-36.

[29] Krishnamurthy J, Torrice C, Ramsey MR, et al. Ink4a/Arf expression is a biomarker of aging. J Clin Invest 2004; 114:1299-307.

[30] García-Cao I, García-Cao M, Martín-Caballero J, et al. "Super p53" mice exhibit enhanced DNA damage response, are tumor resistant and age normally. Embo J 2002; 21:6225-35.

[31] Sanz-González SM, Barquín L, García-Cao I, et al. Increased p53 gene dosage reduces neointimal thickening induced by mechanical injury but has no effect on native atherosclerosis. Cardiovasc Res 2007; 75:803-12.

[32] Janzen V, Forkert R, Fleming HE, et al. Stem-cell ageing modified by the cyclin-dependent kinase inhibitor $p16^{INK4a}$. Nature 2006; 443:421-6.

[33] Molofsky AV, Slutsky SG, Joseph NM, et al. Increasing $p16^{INK4a}$ expression decreases forebrain progenitors and neurogenesis during ageing. Nature 2006; 443:448-52.

[34] Collado M, Blasco MA, Serrano M. Cellular senescence in cancer and aging. Cell 2007; 130:223-33.

[35] Chen D, Krasinski K, Sylvester A, et al. Downregulation of cyclin-dependent kinase 2 activity and cyclin a promoter activity in vascular smooth muscle cells by $p27^{KIP1}$, an inhibitor of neointima formation in the rat carotid artery. J Clin Invest 1997; 99:2334-41.

[36] Chang MW, Barr E, Lu MM, et al. Adenovirus-mediated over-expression of the cyclin/cyclin-dependent kinase inhibitor, p21 inhibits vascular smooth muscle cell proliferation and neointima formation in the rat carotid artery model of balloon angioplasty. J Clin Invest 1995; 96:2260-8.

[37] Tanner FC, Boehm M, Akyurek LM, et al. Differential effects of the cyclin-dependent kinase inhibitors $p27^{Kip1}$, $p21^{Cip1}$, and $p16^{Ink4}$ on vascular smooth muscle cell proliferation. Circulation 2000; 101:2022-5.

[38] Yang ZY, Simari RD, Perkins ND, et al. Role of the p21 cyclin-dependent kinase inhibitor in limiting intimal cell proliferation in response to arterial injury. Proc Natl Acad Sci U S A 1996; 93:7905-10.

[39] Díez-Juan A, Pérez P, Aracil M, et al. Selective inactivation of $p27^{Kip1}$ in hematopoietic progenitor cells increases neointimal macrophage proliferation and accelerates atherosclerosis. Blood 2004; 103:158-61.

[40] Díez-Juan A, Andrés V. The growth suppressor $p27^{Kip1}$ protects against diet-induced atherosclerosis. Faseb J 2001; 15:1989-95.

[41] Merched AJ, Chan L. Absence of $p21^{Waf1/Cip1/Sdi1}$ modulates macrophage differentiation and inflammatory response and protects against atherosclerosis. Circulation 2004; 110:3830-41.

FIGURE LEGENDS

Fig 1: Increased *Ink4/Arf* gene dosage moderately increases $p16^{Ink4a}$, $p15^{Ink4b}$ and $p19^{Arf}$ transcript levels and augments UV-induced apoptosis of macrophages. (A) qPCR of liver and aorta from 4-month-old mice fed high-fat diet and 8-month-old mice fed standard chow, respectively. Transcript levels in apoE-/-Super-Ink4/Arf mice are shown relative to apoE-/- (=1). **(B)** Bone marrow–derived macrophages were untreated or irradiated with UV light (80 J/m^2) and harvested after 24h. Apoptotic macrophages were identified by flow cytometry as the sub-G0/G1 population after propidium iodide staining (n=3 independent experiments). Representative plots of UV-treated cells are shown (y-axis: cell counts; x-axis: intensity of fluorescent signal).

Fig.2. Increased *Ink4/Arf* gene dosage does not affect diet-induced atherosclerosis in female apoE-null mice. Female apoE-/- and apoE-/-Super-Ink4/Arf mice were fed a high-fat diet for 10wk (n=8 each genotype). **(A)** Plasma lipid levels before and after fat-feeding (pre-diet and post-diet, respectively). **(B)** Atherosclerosis burden quantified in Oil Red-O-stained aortic arch and thoracic aorta. **(C)** Atherosclerosis burden quantified in hematoxylin/eosin-stained cross-sections of aortic sinus and ascending aorta (average of 4 cross-sections separated by ~6 μm) Atherosclerotic plaques are delineated by discontinuous lines.

Fig. 3. Increased *Ink4/Arf* gene dosage does not affect atherosclerotic plaque composition in fat-fed apoE-null mice. Mice were fed a high-fat diet for 10wk, and neointimal content of macrophages (anti-Mac3 immunostaining), VSMCs (anti-SMα-actin immunostaining) and collagen (Masson's trichrome) was quantified in the aortic sinus. Atherosclerotic plaques are delineated by discontinuous lines. **(A)** Female mice (n=8 each genotype). **(B)** Male mice (n=9 apoE-/-, n=8 apoE-/-Super-Ink4/Arf).

Fig.4. Increased *Ink4/Arf* gene dosage does not affect atherosclerosis development in apoE-null mice fed standard chow. Atherosclerosis was analyzed in 8-month-old apoE-/- mice (7 males, 7 females) and apoE-/-Super-Ink4/Arf mice (6 males, 4 females) that were always fed standard chow after weaning. **(A)** Plasma lipid levels. **(B)** Atheroma size in the aortic arch quantified by en-face Oil Red-O staining. **(C)** Atheroma size in aortic sinus quantified in hematoxylin/eosin-stained cross-sections (average of 4 cross-sections separated by ~6 µm). **(D)** Neointimal content of macrophages (anti-Mac3 immunostaining), VSMCs (anti-SMα-actin imunostaining) and collagen (Masson's trichrome) in aortic sinus. Atherosclerotic plaques in cross-sections are delineated by discontinuous lines.

Fig.5 Neointimal cell proliferation and apoptosis in apoE-null mice is not affected by increased *Ink4/Arf* gene dosage. Double immunofluorescence analysis of aortic sinus cross-sections of 8-month-old mice fed standard chow (n=5 each genotype) to quantify neointimal cell proliferation (anti-Ki67) and apoptosis (TUNEL) (atheromata delineated by discontinuous lines). **(A)** Percentage of proliferating macrophages (Ki67-F4/80 double-positive cells) within the F4/80-positive population (green: Ki67; red: F4/80; blue: DAPI). **(B)** Percentage of proliferating VSMCs (Ki67-SMα-actin double-positive cells) within the SMα-actin-positive population (green: Ki67; red: SMα-actin; blue: DAPI). **(C)** Percentage of apoptotic cells (green: TUNEL; red: DAPI). Arrows point to double-positive cells in A and B and to TUNEL-positive nuclei in **(C).**

FIGURE 1

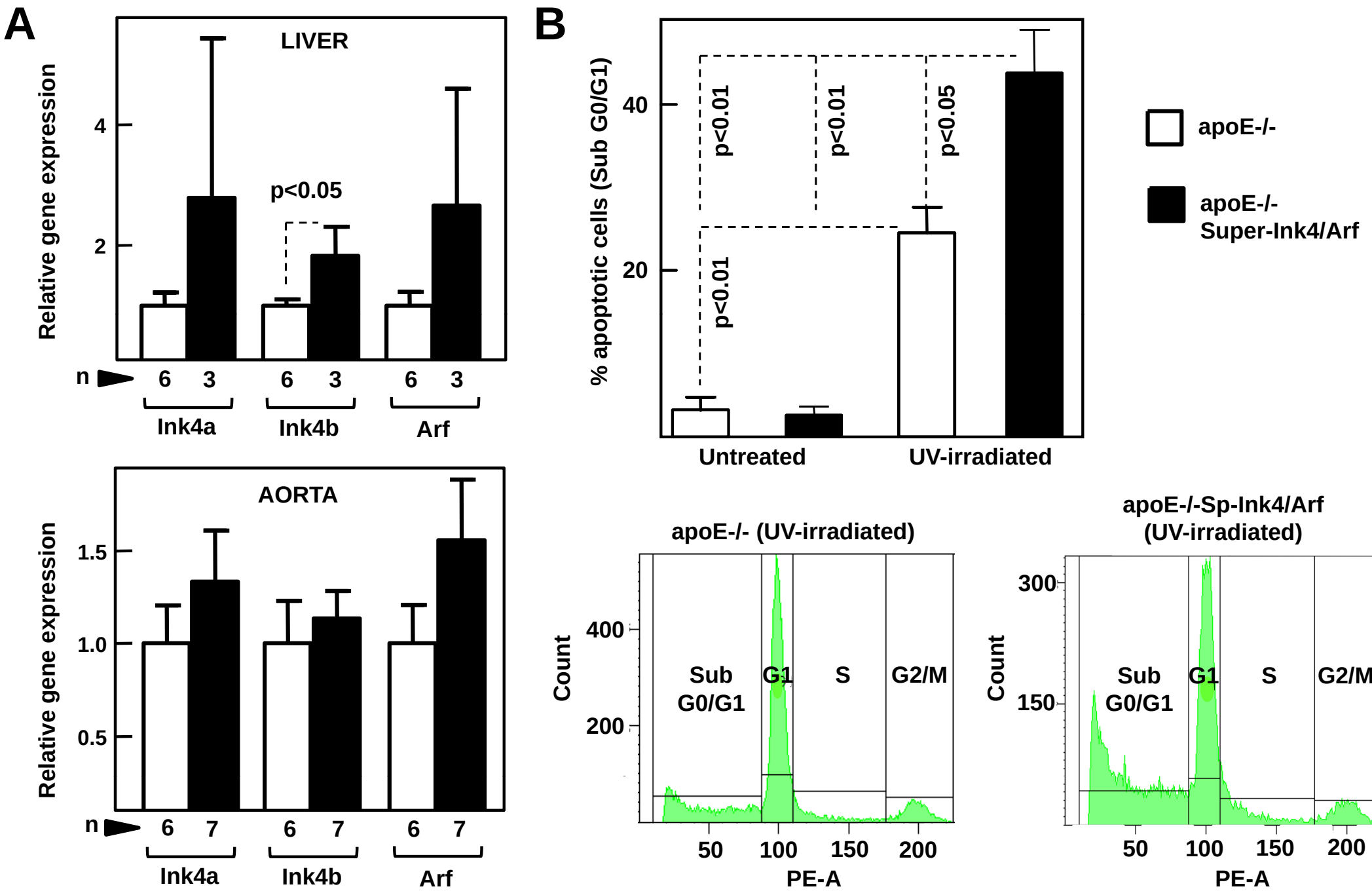
A
LIVER
Relative gene expression
4
2
p<0.05
n
6
3
6
3
6
3
Ink4a
Ink4b
Arf
AORTA
Relative gene expression
1.5
1.0
0.5
n
6
7
6
7
6
7
Ink4a
Ink4b
Arf
B
% apoptotic cells (Sub G0/G1)
40
20
p<0.01
p<0.01
p<0.05
p<0.01
Untreated
UV-irradiated
apoE-/-
apoE-/-
Super-Ink4/Arf
apoE-/- (UV-irradiated)
Count
400
200
Sub
G0/G1
G1
S
G2/M
50
100
150
200
PE-A
apoE-/-Sp-Ink4/Arf
(UV-irradiated)
Count
300
150
Sub
G0/G1
G1
S
G2/M
50
100
150
200
PE-A

FIGURE 2

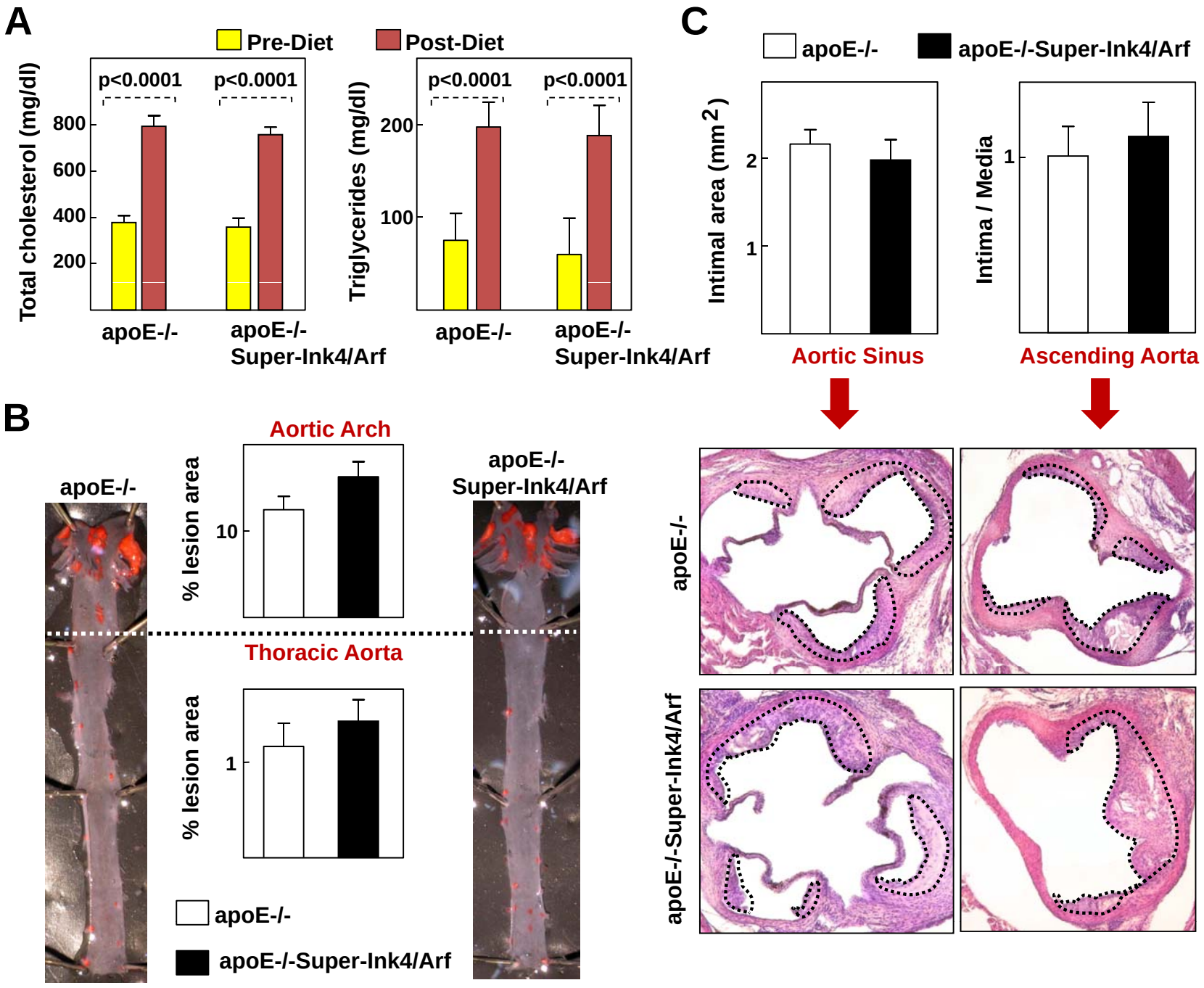
A
Pre-Diet
Post-Diet
Total cholesterol (mg/dl)
p<0.0001
p<0.0001
800
600
400
200
apoE-/-
apoE-/-
Super-Ink4/Arf
Triglycerides (mg/dl)
p<0.0001
p<0.0001
200
100
apoE-/-
apoE-/-
Super-Ink4/Arf
B
apoE-/-
Aortic Arch
% lesion area
10
apoE-/-
Super-Ink4/Arf
Thoracic Aorta
% lesion area
1
apoE-/-
apoE-/-Super-Ink4/Arf
C
apoE-/-
apoE-/-Super-Ink4/Arf
Intimal area (mm2)
2
1
Intima / Media
1
Aortic Sinus
Ascending Aorta
apoE-/-
apoE-/-Super-Ink4/Arf

FIGURE 3

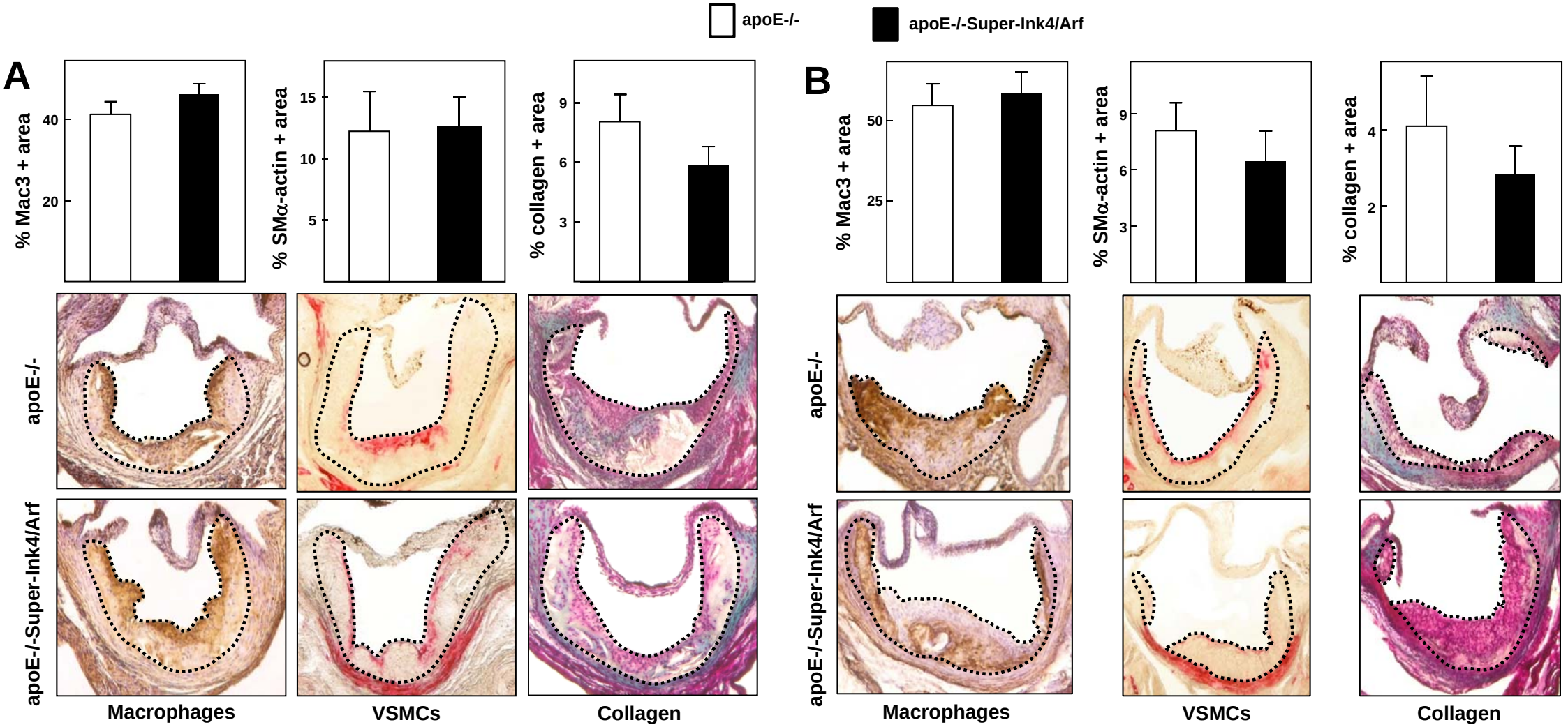
apoE-/-
apoE-/-Super-Ink4/Arf
A
B
% Mac3 + area
% SMα-actin + area
% collagen + area
40
20
15
10
5
9
6
3
50
25
9
6
3
4
2
apoE-/-
apoE-/-Super-Ink4/Arf
Macrophages
VSMCs
Collagen

FIGURE 4

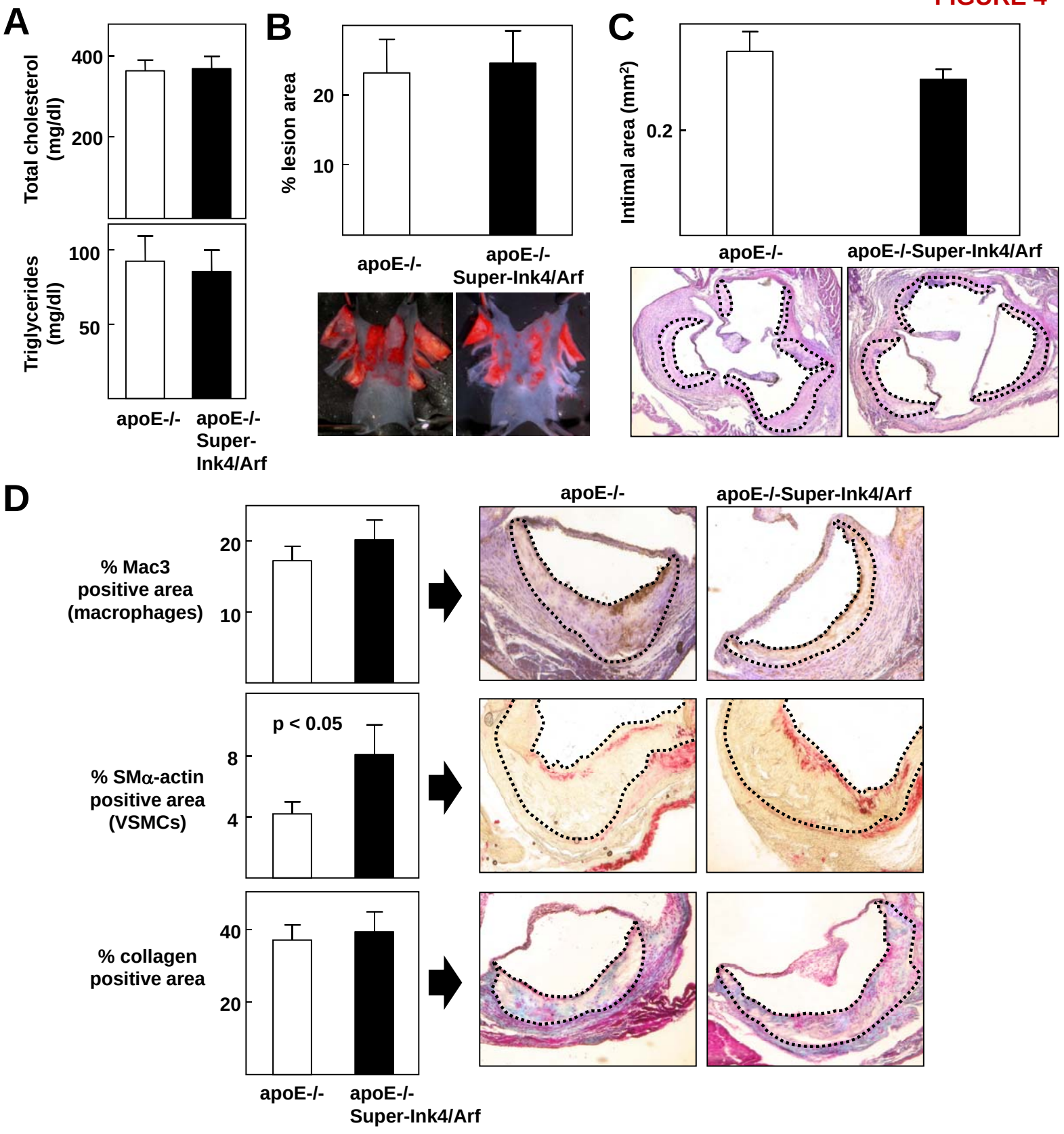
A
Total cholesterol (mg/dl)
400
200
Triglycerides (mg/dl)
100
50
apoE-/-
apoE-/- Super-Ink4/Arf
B
% lesion area
20
10
apoE-/-
apoE-/- Super-Ink4/Arf
C
Intimal area (mm²)
0.2
apoE-/-
apoE-/-Super-Ink4/Arf
D
% Mac3 positive area (macrophages)
20
10
% SMα-actin positive area (VSMCs)
p < 0.05
8
4
% collagen positive area
40
20
apoE-/-
apoE-/-Super-Ink4/Arf
apoE-/-
apoE-/- Super-Ink4/Arf

FIGURE 5

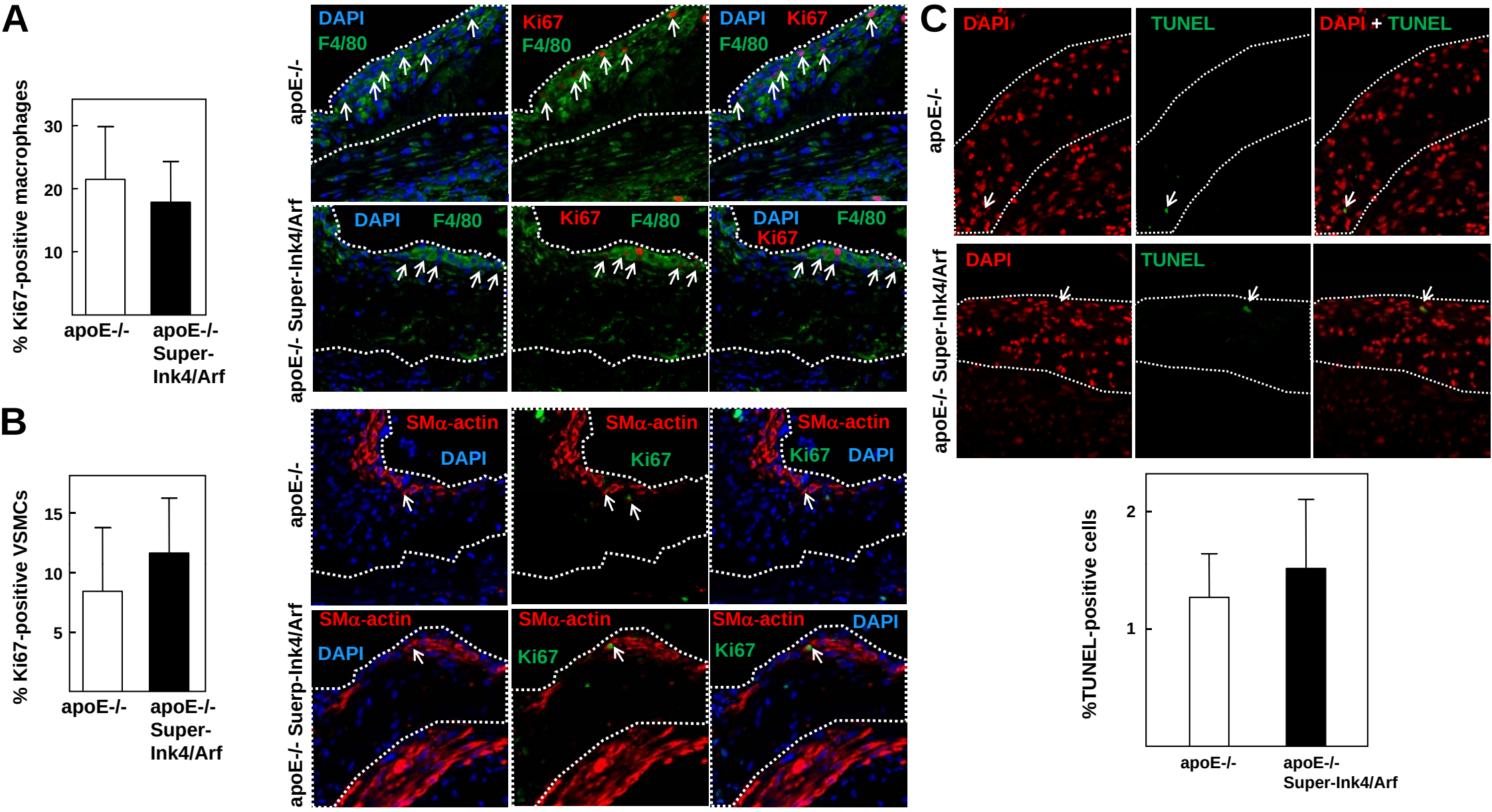
A
% Ki67-positive macrophages
30
20
10
apoE-/-
apoE-/- Super-Ink4/Arf
B
% Ki67-positive VSMCs
15
10
5
apoE-/-
apoE-/- Super-Ink4/Arf
apoE-/-
apoE-/- Super-Ink4/Arf
DAPI
F4/80
Ki67
SMα-actin
C
DAPI
TUNEL
DAPI + TUNEL
%TUNEL-positive cells
2
1
apoE-/-
apoE-/- Super-Ink4/Arf